Structure and Spectra of UO_2F_2 and Its Hydrated Species

Qi Wang and Russell M. Pitzer*

Department of Chemistry, The Ohio State University, 100 West 18th Avenue, Columbus, Ohio 43210

Received: October 31, 2000; In Final Form: May 9, 2001

The electronic spectra of UO_2F_2, both isolated and hydrated, have been studied using ab initio spin−orbit configuration interaction calculations based on relativistic effective core potentials. The structures of UO_2F_2 species were obtained by the density functional theory method. The initial structure has a (nonplanar) C_{2v} geometry, while adding solvating water molecules and optimizing the structure $UO_2F_2(H_2O)_n$ give a very stable structure for $n = 4$, with D_2 geometry. The ground state and some excited states were studied for $UO_2F_2(H_2O)_n$ using the structures obtained. Electric-dipole transition moments were calculated for $UO_2F_2(H_2O)_4$. Spin−orbit and equatorial−ligand (F^-, H_2O) interactions compete in determining the splittings of the known $^3\Delta_g$ state of the uranyl ion, particularly the $^3\Delta_{1g}$ luminescent state.

Introduction

Uranyl fluoride (UO_2F_2) is a uranyl compound that draws substantial attention in uranium chemistry since it is a product of the reaction of UF_6 with moisture. The U.S. Department of Energy currently stores 560 000 metric tons of uranium hexafluoride (UF_6) in 46 500 cylinders in Ohio, Kentucky, and Tennessee.[1] Because the ^{235}U isotope has been substantially removed from this material, it is usually referred to as depleted uranium hexafluoride (DUF_6). A number of the DUF_6 storage cylinders are corroding, and a few of them have leaked. When DUF_6 cylinders leak, atomspheric water reacts with the stored UF_6 and uranyl fluoride (UO_2F_2) is the primary uranium species that forms:[2]

$$UF_6 + 2H_2O \rightarrow UO_2F_2 + 4HF \qquad (1)$$

Investigation of the speciation of electronically excited uranyl fluoride complexes has shown that most of the luminescence in acidic HF solutions of uranyl fluorides arises[3] from electronically excited $UO_2F_2(H_2O)_n$. Thus, luminescence detection of UO_2F_2 is potentially a rapid, highly sensitive method for the detection of leaking UF_6 cylinders, and the study of the fluorescence of UO_2F_2 is of particular interest.

Enhancement of uranyl luminescence in aqueous solution by means of F^- ions has long been exploited for analytical purposes. The study of Kaminski et al.[4] provides an example of such work, and they cite early analytical studies. Moriyasu et al.[5] carried out a systematic study of the influence of fluoride on luminescence lifetimes. They reported that the uranyl luminescence decay rate at 298 K decreased with increasing fluoride concentration to a certain value and then remained constant, and they concluded that hydrated UO_2F_2, $UO_2F_3^-$, and $UO_2F_4^{2-}$ have the same luminescence lifetimes. Although there remain some controversial arguments on the nature of the luminescing state (or states) of uranyl and its complexes,[6−8] Beitz and Williams[3] investigated the speciation of electronically excited uranyl fluoride complexes and found that the longest lifetime was observed from uranyl in 1M HF + 1M $HClO_4$. Using a luminescence dynamics model that assumes equilibrium among elctronically excited uranyl fluoride species and free fluoride ions, they attributed this long-lived uranyl luminescence in aqueous solution primarily to hydrated UO_2F_2.

At certain fluoride concentrations, biexponential[5,9,10] decay curves have been observed for the emission of $UO_2F_4^{2-}$ in aqueous solution. This behavior has been interpreted in terms of the formation of different fluoro complexes[5,10] or exciplexes.[9] Formosinho and Miguel[11] postulate a reversible crossing mechanism between two almost isoenergetic excited-state species U* and X*. Their spectroscopic results suggest that X* is located 300 cm^{-1} lower than U*.[12] An initial proposal[11−13] was that U* and X* are simply different electronic states of the same $[UO_2(H_2O)_5]^{2+}$ species. However, Marcantonatos[14] pointed out that it is difficult to explain the biexponential decay in terms of emission from two states of the same species, as this would imply that emission is faster than the nonradiative transition between these states. The alternative explanation is that U* and X* refer to excited states of different uranyl complexes. Burrows et al.[15] assigned U* to $*[UO_2(H_2O)_6]^{2+}$ and X* to $*[UO_2(H_2O)_5]^{2+}$ and attributed their equilibrium to this process. Billing et al.[6] claim that the two emitting $UO_2F_4^{2-}$ species are coupled by a "reversible crossing mechanism" based on their "resolving" their observed emission spectrum into two sets of vibronic progressions with some other observations. Baird and Kemp[16] reviewed this work with a good summary of the different mechanisms. Most arguments favor two different luminescent chemical species in solution (possibly a dimer or an additional water of hydration as already mentioned) rather than two luminescent states of the same chemical species. UO_2F_2 is known to dimerize in solution at moderate concentration.[17]

Low-temperature spectroscopic absorption studies of salts of uranyl chlorides and acetates have shown evidence that the splitting between the lowest-lying excited electronic state of uranyl and the next higher-lying excited state in such compounds amounts to only a few to a few tens of wavenumbers.[18] At higher temperatures, following ultraviolet excitation, thermal population of the higher-lying state can give rise to emission of so-called "electronic hot bands".

In our work, we use relativistic quantum chemistry to study the splittings of these lower-lying excited electronic states and the intensities of their transitions to the ground state for $UO_2F_2(H_2O)_n$.

* Corresponding author. E-mail: pitzer.3@osu.edu.

10.1021/jp004009z CCC: $20.00
Published on Web 08/17/2001

TABLE 1: F cc-pVDZ Basis Set: (4s4p1d)/[3s2p1d]/[2s2p1d]

orbital	primitives	contraction	contraction	contraction
s	52.19	−0.0097340	0.0	0.0
	9.339	−0.1336174	0.0	0.0
	1.182	0.6009861	0.0	1.0
	0.3626	0.5077536	1.0	0.0
p	22.73	0.0448314	0.0	
	4.986	0.2355939	0.0	
	1.347	0.5089400	0.0	
	0.3472	0.4578876	1.0	
d	1.691	1.0		

TABLE 2: O cc-pVDZ Basis Set: (4s4p1d)/[3s2p1d]/[2s2p1d]

orbital	primitives	contraction	contraction	contraction
s	41.04	−0.0095512	0.0	0.0
	7.161	−0.1334986	0.0	0.0
	0.9074	0.5985186	0.0	1.0
	0.2807	0.5094281	1.0	0.0
p	17.72	0.0430232	0.0	
	3.857	0.2287623	0.0	
	1.046	0.5090575	0.0	
	0.2752	0.4604006	1.0	
d	1.215	1.000000		

Methods

When treating systems which include heavy elements such as uranium, we must both include relativistic effects and treat large numbers of electrons. The problem is addressed by the use of the relativistic effective core potential (RECP) approximation and spin−orbit configuration interaction (CI)[19−21] implemented by the graphical unitary group approach (GUGA).[22,23]

The RECPs used are those developed by Christiansen et al.[24,25] The core electrons are replaced by a potential derived from Dirac−Fock atomic calculations, and thus, we need to treat only the valence electrons explicitly. The atomic calculations also simultaneously produce valence spin−orbit operators at the same level of approximation. The oxygen core and fluoride core are the 1s shell (2 electrons), and the uranium core is the 1s through 5p shells (68 electrons). Thus in UO_2F_2, 76 electrons (core) are not treated explicitly, and 50 electrons (valence) are treated explicitly.

We have developed our own (contracted Gaussian) AO basis sets. Basis sets for effective core potential calculations describe (valence) pseudo-orbitals, which are small in the core region.[26] Choosing correlating orbitals by freeing the most diffusive primitives, as is usually and successfully done for all-electron basis sets, does not produce orbitals which are small in the core region for s orbitals.[26,27] It has been found[27] that an efficient way to arrange the s contractions is to free the two most diffuse s primitives for SCF or MCSCF calculations and then delete the resulting high-energy virtual MO before any extensive correlated calculations are performed. The basis sets were derived in the correlation-consistent manner;[28,29] the resulting F and O basis sets are shown in Tables 1 and 2 and are of (4s4p1d)/[3s2p1d]/[2s2p1d] size, where this notation represents (primitives)/[contractions for determining MOs]/[contractions for correlation calculations]. The hydrogen basis set for the calculation of hydrated species was taken from Dunning;[28] the polarization functions were omitted, so the H basis is of size (4s)/[2s].

The molecular orbitals were obtained from MCSCF calculations, which are carried out on the average of the states we were interested in and did not include the spin−orbit interation. We then performed multireference spin−orbit configuration interation (SOCI) calculations based on the GUGA formalism, as implemented in the COLUMBUS system of quantum chemistry computer programs.[30] The wave functions obtained were used to calculate the electric-dipole transition moments.

The optimization of the geometrical structures was done by density functional theory (DFT). Since our primary purpose was to obtain accurate geometries, the exchange-correlation functional we used is that of the local density approximation (LDA) as implemented in the NWChem system of quantum chemistry computer programs.[31] As discussed later, symmetry constraints were used for complexes with two or three water molecules, but not for the complex with four water molecules.

In the calculation for the bare molecule, we took $3\sigma_u^1\,1\delta_u^1$ and $3\sigma_u^1\,1\phi_u^1$ as reference configurations, and 16 electrons (including the $3\sigma_u$, $3\sigma_g$, $1\pi_g$, and $2\pi_u$ electrons on the uranyl and the electrons in two MOs with mixed F and uranyl character) were correlated. The sizes of the calculations were about 4.8 million double group functions (dgf). In the calculation for the hydrated molecule, this kind of correlation would make the calculations too expensive to be realized, so we froze all the ligand electrons and only correlated the six $2\pi_u$ and $3\sigma_u$ electrons. The size of these calculations was 1.2 million dgf.

TABLE 3: Ground-State Uranyl Fluoride SCF Mulliken Population Analysis

	gross atomic populations					
atom	s	p	d	f	g	total
U	2.123	5.842	11.749	2.222	0.004	21.940
O	3.812	9.047	0.035	0.000	0.000	12.894
F	3.941	11.219	0.005	0.000	0.000	15.165

TABLE 4: MRCISD Results for the Lower Excited States of UO_2F_2

T_e (cm^{-1})	state	Λ-*S* term (configuration)	double group symmetry
0	0_g^+	$^1\Sigma_g^+$ ($3\sigma_u^2$)	A_1
18628	1_g	87% $^3\Delta$ ($3\sigma_u^1 1\delta_u^1$)	A_2
18652	1_g	88% $^3\Delta$ ($3\sigma_u^1 1\delta_u^1$)	B_1
18967	2_g	75% $^3\Delta$+14% $^3\Phi$ ($3\sigma_u^1 1\delta_u^1$)	B_2
20465	2_g	57% $^3\Delta$+32% $^3\Phi$ ($3\sigma_u^1 1\delta_u^1$)	A_1
21176	3_g	57% $^3\Delta$+25% $^3\Phi$ ($3\sigma_u^1 1\delta_u^1$)	B_1
21278	3_g	60% $^3\Delta$+21% $^3\Phi$ ($3\sigma_u^1 1\delta_u^1$)	A_2
22626	2_g	13% $^3\Delta$+73% $^3\Phi$ ($3\sigma_u^1 1\phi_u^1$)	B_2
22838	2_g	30% $^3\Delta$+54% $^3\Phi$ ($3\sigma_u^1 1\phi_u^1$)	A_1
25031	3_g	33% $^3\Delta$+51% $^3\Phi$ ($3\sigma_u^1 1\phi_u^1$)	B_1
25100	3_g	30% $^3\Delta$+52% $^3\Phi$ ($3\sigma_u^1 1\phi_u^1$)	A_2
27281	4_g	88% $^3\Phi$ ($3\sigma_u^1 1\phi_u^1$)	A_1
27284	4_g	89% $^3\Phi$ ($3\sigma_u^1 1\phi_u^1$)	B_2

Results and Discussion

The inital structure of isolated UO_2F_2 was obtained using the DFT method by D. A. Dixon.[32] This structure is nonplanar and has C_{2v} symmetry. The UO distance is 1.775 Å, the UF distance is 2.039 Å, and the O−U−O angle is 169.51 °, which is 10.49° smaller than the 180° in the linear geometry; the F−U−F angle is 109.67°, essentially the tetrahedral angle.

Our self-consistent-field (SCF) calculation shows that UO_2F_2 is a closed-shell system and that the bonding in it is very similar to that of uranyl.[33] The $3\sigma_g$ (a_1), $3\sigma_u$ (b_1), $1\pi_g$ ($a_2 + b_1$), and $2\pi_u$ ($a_1 + b_2$) occupied MOs are approximately degenerate and higher in energy than the other MOs. They have a considerable mixing of U 6d and 5f atomic orbitals, with the $3\sigma_u$ (b_1) having the largest U 5f mixing; the population of U 5f in $3\sigma_u$ is 0.655 (32.8% 5f character). The overall population analysis is given in Table 3 and corresponds to $U^{+2.06}(O^{-0.45})_2(F^{-0.58})_2$.

If the uranyl ion is rigidly linear and the fluoride bonding is completely ionic, we would expect the F−U−F angle to be

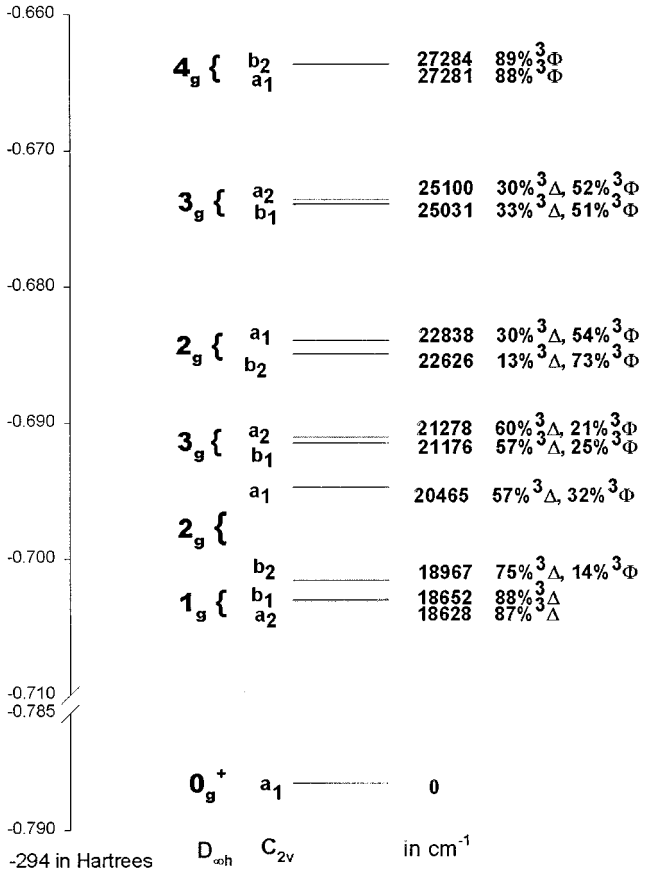

Figure 1. Electronic energy levels of isolated UO_2F_2.

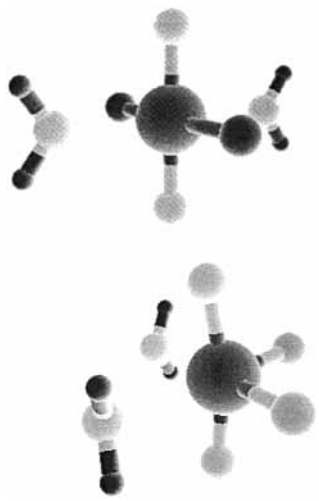

Figure 2. $UO_2F_2(H_2O)_2$ optimized structures. Top: trans fluorides are out of the plane of the page. Bottom: cis fluorides are out of the plane of the page.

180°; on the other hand, if both the O and F ions are comparably ionically bonded, then we would expect a tetrahedral structure. With the U−O bonds being much stronger and shorter than the U−F bonds, the uranyl angle is only moderately bent, but the F−U−F is close to tetrahedral. With a long U−F distance, the F orbitals principally overlap with the U 6d rather than the U 5f orbitals, and this 6d mixing causes the magnitude of the F population to be less than 1.

At the SCF level, where there is no spin−orbit coupling in the calculations, the $^3\Delta_g$ state is lower than the $^3\Phi_g$ by a small amount, indicating that the δ_u orbital is lower than the ϕ_u. This agrees with previous work.[33] The results of the CI calculations

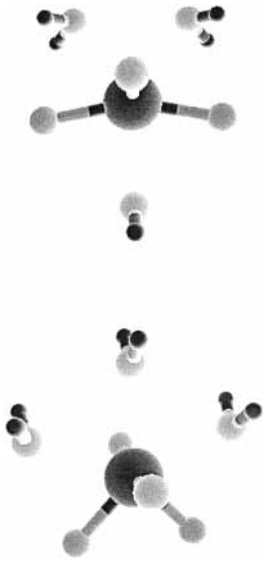

Figure 3. $UO_2F_2(H_2O)_3$ optimized structures. Top: trans fluorides are in the plane of the page. Bottom: cis fluorides are in the plane of the page.

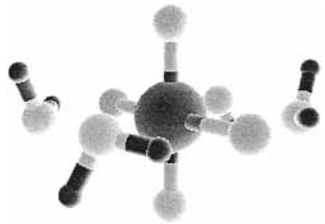

Figure 4. $UO_2F_2(H_2O)_4$ optimized structure. Fluorides are out of the plane of the page.

TABLE 5: MRCISD Results for the Lower Excited States of $UO_2F_2(H_2O)_3$

T_e (cm^{-1})	state	Λ-*S* term (configuration)	double group symmetry	f (10^{-7})
0	0_g^+	$^1\Sigma_g^+$ ($3\sigma_u^2$)	A_1	
18790	1_g	91% $^3\Delta$ ($3\sigma_u^1 1\delta_u^1$)	A_2	0
18797	1_g	91% $^3\Delta$ ($3\sigma_u^1 1\delta_u^1$)	B_1	3.3
19541	2_g	83% $^3\Delta$+8% $^3\Phi$ ($3\sigma_u^1 1\delta_u^1$)	A_1	0.1
20500	2_g	83% $^3\Delta$+8% $^3\Phi$ ($3\sigma_u^1 1\delta_u^1$)	B_2	26.2
21523	3_g	74% $^3\Delta$+14% $^3\Phi$ ($3\sigma_u^1 1\delta_u^1$)	A_2	0
21638	3_g	78% $^3\Delta$+ 9% $^3\Phi$ ($3\sigma_u^1 1\delta_u^1$)	B_1	2.2
24243	2_g	6% $^3\Delta$+78% $^3\Phi$ ($3\sigma_u^1 1\phi_u^1$)	B_2	9.8
24465	2_g	7% $^3\Delta$+80% $^3\Phi$ ($3\sigma_u^1 1\phi_u^1$)	A_1	144.7
26291	3_g	17% $^3\Delta$+67% $^3\Phi$ ($3\sigma_u^1 1\phi_u^1$)	A_2	0
27097	3_g	7% $^3\Delta$+62% $^3\Phi$ ($3\sigma_u^1 1\phi_u^1$)	B_1	108.0
29497	4_g	90% $^3\Phi$ ($3\sigma_u^1 1\phi_u^1$)	B_2	93.5
29547	4_g	90% $^3\Phi$ ($3\sigma_u^1 1\phi_u^1$)	A_1	176.8

are shown in Table 4. We can see that spin−orbit coupling splits both states but splits $^3\Phi$ more than $^3\Delta$. The 2_g and 3_g states show substantial mixing of the $^3\Delta$ and $^3\Phi$ terms. The fluorides break the symmetry, and thus, each spin−orbit state is further split into two states. The order of the interactions is the same as it found by our group[34] for other actinyl complexes:

ax. field (σ,π) > el. rep. > spin−orbit > ax. field (δ,ϕ) + eq. field

For the fluorescent state ($^3\Delta_{g1}$), the splitting from the equatorial field is ca. 24 cm^{-1}; the largest splitting occurs for the 2_g state from the $3\sigma_u^1 1\delta_u^1$ configuration, ca. 1498 cm^{-1}. Other splittings vary from 1 to 175 cm^{-1}. The calculated splitting for the fluorescent state (24 cm^{-1}) is similar in magnitude to those found experimentally in crystal spectra.[18] We continued

TABLE 6: $UO_2F_2(H_2O)_n$ DFT Results

no. of H_2O	2		3		4
structure	cis	trans	cis	trans	−
geometry	C_{2v}	C_{2v}	C_{2v}	C_{2v}	D_2
total DFT energy (a.u.)	−976.7179	−976.7180	−1052.6251	−1052.6478	−1128.5955
trans vs cis (cm^{-1})	17	0	4970	0	−
binding energy of H_2O (kcal/mol)	−	−	−	18	26
U−O distance (Å)	1.795	1.791	1.812	1.794	1.775
U−F distance (Å)	2.082	2.066	2.068	2.120	2.315
U−O (H_2O) distance (Å)	2.474	2.457	2.535	2.535, 2.450	2.497
O−U−O angle (°)	167.05	177.63	160.45	174.43	180.00
F−U−F angle (°)	107.58	180.00	86.14	157.60	180.00
imaginary modes	2	3	5	6	0

our work by adding solvating water molecules and optimizing the structures.

When dissolved in aqueous systems, uranyl ions complex readily with H_2O. Uranium in its formal oxidation state of six usually forms strong and short (∼1.7−1.8 Å) covalent bonds with the two axial oxygens and is usually bonded to four to six equatorial ligands at much longer distances through a weaker electrostatic interaction.[35]

There are a number of X-ray crystallographic studies of monomeric, dimeric, and trimeric uranyl compounds containing both fluoride ions and water molecules,[36] with many not having water molecules bound to the uranyl moieties. For such monomeric uranyl complexes with a water molecule in the equatorial position, there is an X-ray study[37] and an EXAFS study.[38] Standard equatorial distances are[36] 2.23 Å for U−F and 2.35 Å for U−OH_2; H bonding with more distant molecules affects these values noticeably.[37] We used density functional methods to study trends in the structures, vibrational frequencies, and binding energies of UO_2F_2 complexes with 2−4 equatorial water molecules.

We first added two H_2O molecules to the initial structure of UO_2F_2, considering both trans and cis geometries. The optimized structures are shown in Figure 2. The results show that the two geometries are quite close in energy (17 cm^{-1} difference) and they both have vibrational modes with imaginary frequencies which correspond to water molecules rotating in the equatorial plane. Thus our structures are not at minima, but optimizing the water molecule positions further yields little additional energy.[39] Water ligand rotation also suggests that more ligands may be possible, so we added a third water molecule, also with two geometries. The cis optimized structure is higher in energy than trans by about 5000 cm^{-1}, and there are still imaginary frequencies for both geometries. For both of these structures (two waters and three waters), the geometries have C_{2v} symmetry. The $UO_2F_2(H_2O)_3$ optimized structures are shown in Figure 3.

In Table 5, we give the calculated electric-dipole transition intensities for electronic transitions in $UO_2F_2(H_2O)_3$. The largest ones primarily involve the U 5fϕ orbitals, which are intrinsically of ungerade symmetry ($1\phi_u$) but are known[40] to be mixed by a 5-fold field with the U 6dδ_g orbitals as is needed for a larger intensity in an excitation from an intrinsically ungerade orbital ($3\sigma_u$).

After we added the fourth water, the optimization gave no imaginary modes, indicating a minimum. The six-coordinate structure clearly shows that there is strong hydrogen bonding with the fluoride ions and that this is what stablizes this structure. The binding energies of the third and fourth water are 18 and 26 kcal/mol respectively, although use of a different exchange-correlation functional, such as B3LYP,[41] would be needed for good DFT energies. This final structure, as shown in Figure 4, has D_2 symmetry. All of this optimization work is summarized in Table 6.

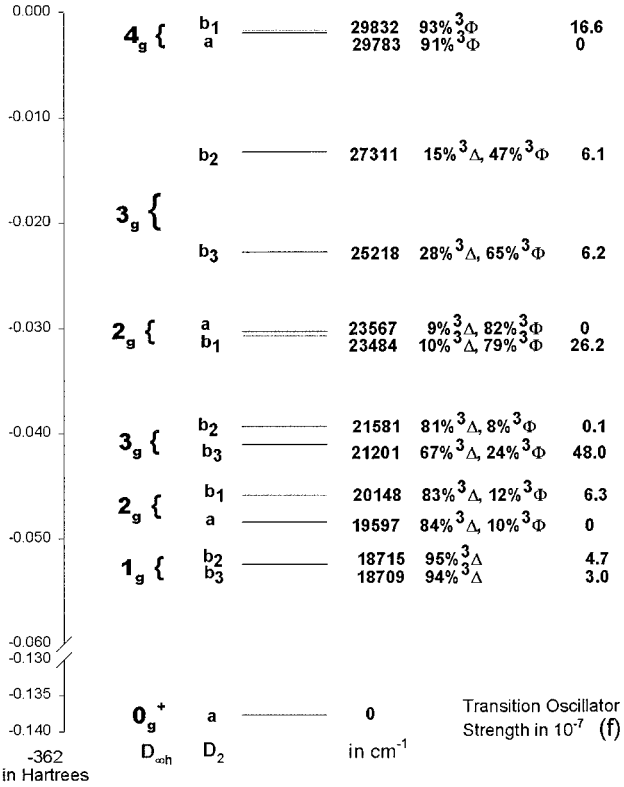

Figure 5. Electronic energy levels of $UO_2F_2(H_2O)_4$.

TABLE 7: MRCISD Results for the Lower Excited States of $UO_2F_2(H_2O)_4$

T_e (cm^{-1})	state	Λ-*S* term (Configuration)	double group symmetry	*f* (10^{-7})
0	0_g^+	$^1\Sigma_g^+$ ($3\sigma_u^2$)	A	
18709	1_g	94% $^3\Delta$ ($3\sigma_u^1 1\delta_u^1$)	B_3	3.0
18715	1_g	95% $^3\Delta$ ($3\sigma_u^1 1\delta_u^1$)	B_2	4.7
19597	2_g	84% $^3\Delta$+10% $^3\Phi$ ($3\sigma_u^1 1\delta_u^1$)	A	0
20148	2_g	83% $^3\Delta$+12% $^3\Phi$ ($3\sigma_u^1 1\delta_u^1$)	B_1	6.3
21201	3_g	67% $^3\Delta$+24% $^3\Phi$ ($3\sigma_u^1 1\delta_u^1$)	B_3	48.0
21581	3_g	81% $^3\Delta$+ 8% $^3\Phi$ ($3\sigma_u^1 1\delta_u^1$)	B_2	0.1
23484	2_g	10% $^3\Delta$+79% $^3\Phi$ ($3\sigma_u^1 1\phi_u^1$)	B_1	26.2
23567	2_g	9% $^3\Delta$+82% $^3\Phi$ ($3\sigma_u^1 1\phi_u^1$)	A	0
25218	3_g	28% $^3\Delta$+65% $^3\Phi$ ($3\sigma_u^1 1\phi_u^1$)	B_3	6.2
27311	3_g	15% $^3\Delta$+47% $^3\Phi$ ($3\sigma_u^1 1\phi_u^1$)	B_2	6.1
29783	4_g	91% $^3\Phi$ ($3\sigma_u^1 1\phi_u^1$)	A	0
29832	4_g	93% $^3\Phi$ ($3\sigma_u^1 1\phi_u^1$)	B_1	16.6

The CI calculated results for $UO_2F_2(H_2O)_4$ were done in the same way as those for UO_2F_2 and are given in Table 7; the corresponding energy levels are plotted in Figure 5. Comparing with the spectrum for the isolated molecule, we find that the energy difference between the highest $^3\Phi$ state and the lowest

$^3\Delta$ state is larger for the hydrated molecule, 11 000 cm^{-1} compared to less than 9000 cm^{-1} for isolated UO_2F_2. For the $^3\Phi_{3g}$ state, there is only 15% $^3\Delta$ and 47% $^3\Phi$, so there is significant mixing from higher excited states (for example, $^1\Phi$). Equatorial−ligand (F^-, H_2O) interactions also split the states, but the effect is smaller than that of the spin−orbit interaction, as it was for the isolated molecule. For the luminescent state $^3\Delta_{1g}$, the splitting is only about 6 cm^{-1}, which is smaller than that of the isolated molecule (24 cm^{-1}) but of the same magnitude. The splittings from equatorial−ligand interactions again range from 6 to 2093 cm^{-1}. The biggest splitting occurs for the $^3\Phi_{3g}$ state (2093 cm^{-1}), while all other splittings are less than 600 cm^{-1}. This is a reasonable result according to the crystal field model[42] for 6-fold coordination. Another reason contributing to the biggest splitting is presumably because of the mixing of higher excited states, as discussed above.

In Table 7, we also list the electric-dipole transition intensities for the electronic spectra of $UO_2F_2(H_2O)_4$. All the electric-dipole oscillator strengths are on the order of 10^{-7} to 10^{-6}, which is quite small, with the biggest one being that for the fifth transition. No experimental data are yet available for comparison, but intensities in $Cs_2UO_2Cl_4$ were assigned to magnetic dipole and electric quadrupole mechanisms.[43]

Conclusion

The electronic spectrum of UO_2F_2, one of the chemcial compounds in nuclear waste, was studied in both isolated and hydrated forms, and their structures were optimized. The splittings caused by the equatorial−ligand interaction vary from a few centimeters^{-1}to a few thousand centimeters^{-1}; for the luminescent state it is only on the order of 10^1 cm^{-1}. The effects of axial and equatorial ligands on the splittings of the electronic states were determined and compared.

Thus, the biexponential decay curves observed may not be interpreted in terms of two excited states from one species, and the underlying mechanism is most likely due to two different luminescent chemical species in solution (possibly a dimer or an additional water of hydration).

Electric-dipole transition intensities were computed for several of the complexes. The values for the oscillator strength of the luminescent state were on the order of 5×10^{-7}, so other intensity mechanisms need to be considered.

Acknowledgment. We thank J. Beitz, A. Pires de Matos, J. Blaudeau, S. Brozell, J. Li, S. Matsika, and V. Vallet for helpful discussions. We thank Z. Zhang for extensive aid with the DFT calculations. We thank Argonne National Laboratory (ANL) for support from their Actinide Synchrotron Studies project and Pacific Northwest National Laboratory (PNNL) for support through Contract 200210, U. S. Department of Energy, the Mathematical, Information, and Computational Science Division, High-Performance Computing and Communications Program of the Office of Computational and Technology Research. PNNL is operated by Battelle Memorial Institute under Contract DE-AC06-76RLO 1830. This work was also supported in part by Contract DE-FG02-01ER15136, U. S. Department of Energy. We used computational facilities at Ohio State University (largely provided by the PNNL grant). The DFT calculations were performed at the Molecular Science Computing Facility at PNNL.

References and Notes

(1) Lawrence Livermore National Laboratory and Science Applications International Corporation. *Depleted Uranium Hexafluoride Management Program, Summary of the Technology Assessment Report for the Long-Term Management of Depleted Uranium Hexafluoride*; Department of Energy; Washington, DC, 1995; p 2.

(2) See http://anchi8.chm.anl.gov/heavy-element/photophysics/duf6.html for the detailed story of storage problems of DUF_6 cylinders and pictures of leaking tanks.

(3) Beitz, J. V.; Williams, C. W. *J. Alloys Compd.* **1997**, *250*, 375−379.

(4) Kaminski, R.; Purcell, F. J.; Russavage, E. *Anal. Chem.* **1981**, *53*, 1093−1096.

(5) Moriyasu, M.; Yokoyama, Y.; Ikeda, S. *J. Inorg. Nucl. Chem.* **1977**, *39*, 2199−2203.

(6) Billing, R.; Zakharova, G. V.; Atabekyan, L. S.; Henning, H. *J. Photochem. Photobiol. A: Chem.* **1991**, *59*, 163−174.

(7) Moulin, C.; Decabox, P.; Trecani, L. *Anal. Chim. Acta* **1996**, *321*, 121−126.

(8) Azenha, M. E. D. G.; Burrows, H. D.; Formosinho, S. J.; Miguel, M. G. M.; Daramanyan, A. P.; Khudyakov, I. V. *J. Lumin.* **1991**, *48/49*, 522−526.

(9) Deschaux, M.; Marcantonatos, M. D. *J. Inorg. Nucl. Chem.* **1981**, *43*, 361−367.

(10) Alfonichev, D. D.; Khamidullina, L. A.; Mamykin, A. V.; Kazakov, V. P. *Radiochemistry* **1986**, *28*, 644−647.

(11) Formosinho, S. J.; Miguel, M. da G. M. *J. Chem. Soc., Faraday Trans. 1* **1984**, *80*, 1745−1756.

(12) Formosinho, S. J.; Miguel, M. da G. M.; Burrows, H. D. *J. Chem. Soc., Faraday Trans. 1* **1984**, *80*, 1717−1733.

(13) Miguel, M. da G. M.; Formosinho, S. J.; Cardoso, A. C.; Burrows, H. D. *J. Chem. Soc., Faraday Trans. 1* **1984**, *80*, 1735−1744.

(14) Marcantonatos, M. D. *J. Inorg. Nucl. Chem.* **1978**, *26*, 41−46.

(15) Burrows, H. D.; Miguel, M. da G. M.; Formosinho, S. J.; Cardoso, A. C. *J. Chem. Soc., Faraday Trans. 1* **1985**, *81*, 49−60.

(16) Baird, C. P.; Kemp, T. J. *Prog. React. Kinet.* **1997**, *22*, 87−139.

(17) Johnson, J. S.; Kraus, K. A.; Young, T. F. *J. Am. Chem. Soc.* **1954**, *76*, 1436−1443.

(18) Jørgensen, C. K.; Reisfeld, R. *Struct. Bonding (Berlin)* **1982**, *50*, 121−171. See Table 2 for crystal splittings of excited states.

(19) Ermler, W. C.; Ross, R. B.; Christiansen, P. A. *Adv. Quantum Chem.* **1988**, *19*, 139−182.

(20) Dolg, M.; Stoll, H. Electronic Structure Calculations for Molecules containing Lanthanide Atoms. In *Handbook on the Physics and Chemistry of Rare Earths*; Gschneider, K. A., Eyring, L., Eds.; Elsevier: Amsterdam, 1995; 607−729.

(21) Balasubramanian, K. *Relativistic Effects in Chemistry: Part A, Theory and Techniques*; Wiley: New York, 1997.

(22) Morokuma, K.; Yamashita, K.; Yabushita, S. Potential Energy Surfaces of Several Elementary Chemical Reactions. In *Supercomputer Algorithms for Reactivity, Dynamics and Kinetics of Small Molecules*; A. Laganà, Ed.; Kluwer: Dordrecht, 1989; pp 37−56.

(23) Yabushita, S.; Zhang, Z.; Pitzer, R. M. *J. Phys. Chem. A* **1999**, *103*, 5791−5800.

(24) See http://www.clarkson.edu/~pac/reps.html for complete references and a library of potentials.

(25) Ermler, W. C.; Ross, R. B.; Christiansen, P. A. *Int. J. Quantum Chem.* **1991**, *40*, 829−846.

(26) Blaudeau, J.-P.; Brozell, S. R.; Matsika, S.; Zhang, Z.; Pitzer, R. M. *Int. J. Quantum Chem.* **2000**, *77*, 516−520.

(27) Christiansen, P. A. *J. Chem. Phys.* **2000**, *112*, 10070−10074.

(28) Dunning, T. H. *J. Chem. Phys.* **1989**, *90*, 1007−1023, See http://www.emsl. pnl.gov:2080/forms/basisform.html for the H basis set. The *s* exponents were multiplied by 1.44 in the standard way.

(29) Wallace, N. M.; Blaudeau, J.-P.; Pitzer, R. M. *Int. J. Quantum Chem.* **1991**, *40*, 789−796.

(30) See http://www.itc.univie.ac.at/~hans/Columbus/columbus.html for information on the COLUMBUS programs.

(31) See http://www.emsl.pnl.gov/pub/docs/nwchem for information on the NWChem programs.

(32) Dixon, D. A. Private communication, 1997.

(33) Zhang, Z.; Pitzer, R. M. *J. Chem. Phys.* **1999**, *103*, 6880−6886.

(34) Matsika, S.; Zhang, Z.; Brozell, S. R.; Blaudeau, J.-P.; Wang, Q.; Pitzer, R. M. *J. Phys. Chem. A* **2001**, *105*, 3825−3828

(35) Zhang, Z.; Harrison, R. J. Density Functional Study of the Ground States of Aqua Anion UO_2^{2+} Complexes. In *Theory, Modeling, and Simulation 1999 Annual Report*; Dixon, D. A., Eades, R. A., Garrett, B. C., Gracio, D. K., Jones, D. R., Jones-Oliveira, J. B., Nichols, J. A., et al., Eds.; 1999, Chapter 5, pp 14−14.

(36) Dao, N. Q. *Inorg. Chim. Acta* **1984**, *95*, 165−178.

(37) Mak, T. C. W.; Yip, W.-H. *Inorg. Chim. Acta* **1985**, *109*, 131−133.

(38) Vallet, V.; Wahlgren, U.; Schimmelpfennig, B.; Moll, H.; Szabó, Z.; Grenthe, I. *Inorg. Chem.* **2001**, *40*, 3516−3525.

(39) Hay, P. J.; Martin, R. L.; Schreckenbach, G. *J. Phys. Chem. A* **2000**, *104*, 6259−6270.

(40) Matsika, S.; Pitzer, R. M.; Reed, T. D. *J. Phys. Chem. A* **2000**, *104*, 11983−11992.
(41) Becke, A. D. *J. Chem. Phys.* **1993**, *98*, 5648−5652.
(42) Görller-Walrand, C.; Vanquickenborne, L. G. *J. Chem. Phys.* **1972**, *57*, 1436−1440.
(43) Denning, R. G. *Struct. Bonding (Berlin)* **1992**, *79*, 215−271.